A Reactive Power Control Algorithm with Current Limitation in the *abc*-Frame for Inverter-Based Distributed Energy Resources

Aldo M. Rizo, María A. Mantilla, Juan M. Rey
Escuela de Ingeniería Eléctrica, Electrónica y Telecomunicaciones (E3T)
Universidad Industrial de Santander (UIS)
Bucaramanga, Colombia
aldo2248435@correo.uis.edu.co, {marialem, juanmrey}@uis.edu.co

***Abstract*—This paper presents a reactive power control algorithm with current limitation for grid-connected inverters operating under the IEEE 1547-2018 standard modes. The algorithm operates directly in the *abc* frame, avoiding coordinate transformations, and adjusts the inverter reference current for any of the four voltage and reactive power control modes specified in the standard, while also ensuring inverter capacity limits and improving voltage regulation. The control structure combines the proposed algorithm, proportional–resonant regulation, and level-shifted pulse width modulation applied to a three-level NPC multilevel inverter with LCL filter. Simulation results in MATLAB/Simulink demonstrate effective current limitation, as well as control of voltage and reactive power, fulfilling the standard requirements.**

***Index Terms*—Current limitation, voltage and reactive power control, *abc* reference frame, voltage regulation, distributed energy resources (DER), IEEE 1547-2018 standard.**

I. Introduction

The rapid growth in the integration of renewable energy sources, particularly grid-connected photovoltaic systems [1], has highlighted the need for advanced control strategies to ensure system stability, power quality, and compliance with interconnection standards for distributed energy resources (DER) and the electric grid [2]. Power electronic converters have become essential in this framework, enabling new approaches to fulfill grid requirements through their control strategies. The IEEE 1547-2018 standard [3] specifies technical requirements for the operation of grid-connected inverters for DER applications. One of the steady-state operation requirements is voltage and reactive power control, which is intended to improve voltage regulation. To achieve this, the standard defines four mutually exclusive operating modes, each leading to a distinct reactive power control strategy.

In active distribution networks (ADN), various methods exist for reactive power control. One approach is the centralized control, which aims to optimize the reactive power of multiple DERs interconnected within an ADN by considering data such as grid parameters, load dynamics, and renewable energy forecasts. The control decisions are dispatched through a communication system among DERs for optimal operation [2]. In contrast, local control determines in real time the required reactive power based on the voltage measured at the point of common coupling (PCC) to enhance voltage regulation. The reactive power control strategy can operate in several modes; for example, it can be based on Volt-VAR curves applied to power electronic inverters [4]. The operating mode could be defined either by a centralized command of the ADN or according to the DER operator's criteria, as required. Furthermore, to achieve effective local control, it is necessary to comply with inverter power and current capacity limits, as well as with standard requirements to maintain security, stability, and steady-state operational limits [5].

Building upon these advances, this work adopts a local voltage and reactive power control approach implemented directly in the *abc* reference frame, free of coordinate transformations. The proposed method aims to ensure current limitation while guaranteeing grid operator requirements and full compliance with IEEE 1547-2018 operational modes for voltage and reactive power control.

The proposed algorithm dynamically adjusts the inverter reference current according to any of the four operating modes defined in the standard, known as constant reactive power, constant power factor, voltage–reactive power (Volt–VAR), and active–reactive power (Watt–VAR). The algorithm ensures that the reference current remains within the inverter rated capacity by adjusting the active and reactive powers when required according to the operating mode. The strategy is designed considering positive sequence balanced voltages in the PCC, with negligible harmonic distortion.

The algorithm's performance is verified through simulations in MATLAB/Simulink for a grid-connected three-level inverter with LCL filter. The algorithm was evaluated within the four operating modes of the standard in scenarios where the injection or absorption of active power affects voltage regulation; thus, reactive power control is applied to reduce the deviation from steady-state voltage operating limits.

The paper is organized as follows: Section II describes the

This research was supported by Universidad Industrial de Santander with project entitled "Plataforma de evaluación de tecnologías emergentes para la transición energética en el marco de las redes inteligentes de energía eléctrica" project code 4224-2024.

979-8-3315-8138-1

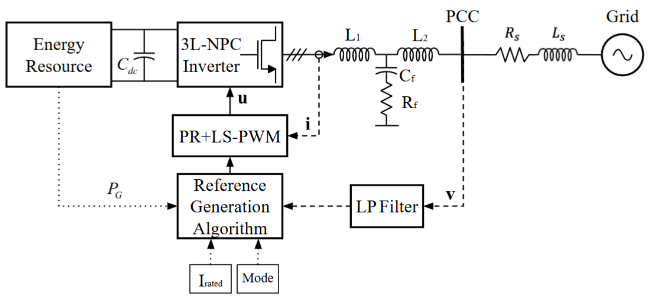

Fig. 1. Simulation system scheme

system overview, including its elements and control system. Section III presents the proposed algorithm for the operating modes defined by the IEEE 1547-2018 standard, considering current limitation. Section IV introduces the case study and discusses the simulation results under different operating scenarios. Finally, Section V provides concluding remarks and future research directions.

II. System Overview

For this study, a system composed of a three-phase three-level (3L) neutral-point-clamped (NPC) inverter is employed. The inverter is connected to the PCC through an LCL filter, which is connected in AC to the electrical grid, represented by a Thévenin equivalent. On the inverter's DC side, a voltage source is connected to represent an energy resource. This source may correspond to a solar photovoltaic plant, a battery bank, an electrolyzer, or a combination of these or other resources that meet the definition of a DER. The proposed scheme is shown in Fig. 1.

The inverter's control system is composed of two loops: a reference current generator and a current controller operating with a pulse-width modulation (PWM) technique. The reference current generator acts based on the measured voltages at the PCC ($\mathbf{v}$), conditioned by a low-pass (LP) filter, the measured inverter current ($\mathbf{i}$), the nominal current capacity (I_{rated}), the generated power (P_G) from the energy resource, and the operating mode (Mode). This algorithm produces a reference current, which is followed using a proportional–resonant (PR) controller. The output of this controller is then synthesized through the level-shifted PWM (LS-PWM) technique to generate the firing pulses for the inverter. The control strategy is explained in the following subsections.

A. PR+LS-PWM

The PR controller in the *abc* reference frame enables the regulation of sinusoidal currents, aiming to achieve negligible steady-state error without coordinate transformations or PLL synchronization [6]. This control loop generates the inverter's output reference voltage to track the desired reference current. Finally, the LS-PWM technique is used to synthesize the reference voltage.

The LS-PWM technique employs multiple triangular carriers of identical frequency and amplitude, vertically shifted to generate the inverter's switching states, which produce multilevel output voltages. The number of carriers corresponds to the number of inverter levels minus one, resulting in a waveform closer to a sinusoid with reduced harmonic content and improved DC-bus utilization [7].

B. Reference current generation

The reference current generation determines the inverter output current needed to control the active and reactive power delivered to the grid. The reference currents in the *abc* reference frame are defined as [8], [9]:

$$\begin{bmatrix} i_a \\ i_b \\ i_c \end{bmatrix} = \underbrace{\frac{p(t)}{v_a^2+v_b^2+v_c^2}\begin{bmatrix} v_a \\ v_b \\ v_c \end{bmatrix}}_{\mathbf{i_p}} + \underbrace{\frac{q(t)}{\sqrt{3}\,(v_a^2+v_b^2+v_c^2)}\begin{bmatrix} v_b - v_c \\ v_c - v_a \\ v_a - v_b \end{bmatrix}}_{\mathbf{i_q}} \quad (1)$$

where v_a, v_b, and v_c are the instantaneous voltages in the PCC, while $p_{(t)}$ and $q_{(t)}$ are the instantaneous active and reactive powers delivered to the grid. As shown in (1), the reference current is composed of two components: an instantaneous active current ($\mathbf{i_p}$) and an instantaneous nonactive current ($\mathbf{i_q}$).

Assuming balanced, purely sinusoidal positive-sequence voltages in the PCC, the RMS line voltage is computed as:

$$V_{L,\text{rms}} = \sqrt{v_a^2+v_b^2+v_c^2}. \quad (2)$$

Under the same ideal PCC voltage conditions, the reference currents correspond to purely sinusoidal positive-sequence signals. Thus, the amplitudes of the instantaneous active and nonactive currents, I_p and I_q, can be calculated as:

$$I_p = \sqrt{\frac{2}{3\,V_{L,\text{rms}}^2}}\,P^*, \qquad I_q = \sqrt{\frac{2}{3\,V_{L,\text{rms}}^2}}\,Q^*, \quad (3)$$

where P^* and Q^* are the reference active and reactive powers to be delivered to the grid. Moreover, the amplitude of the reference current can be expressed as:

$$I_{\text{ref}} = \sqrt{I_p^2+I_q^2} = \sqrt{\frac{2}{3}}\,\frac{\sqrt{P^{*2}+Q^{*2}}}{V_{L,\text{rms}}}. \quad (4)$$

To ensure inverter operation within its rated current capability (I_{rated}), the following current limit condition must be guaranteed:

$$I_{\text{ref}} \leq I_{\text{rated}}. \quad (5)$$

In the following section, a control algorithm is proposed to achieve this condition under the different operating modes defined for voltage and reactive power control.

III. Proposed Reference Generation Algorithm for Inverter Operation Modes

The proposed algorithm governs inverter behavior under the following modes: constant reactive power, Volt–VAR, constant power factor, and Watt–VAR. The objective is to ensure current limitations while maintaining standard-compliant voltage and power control.

979-8-3315-8138-1

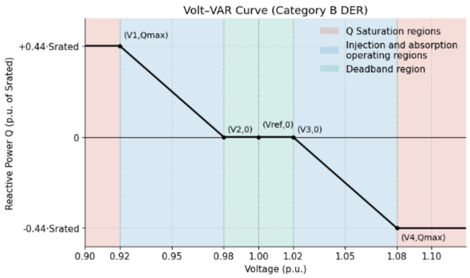

Fig. 2. Volt-VAR Curve.

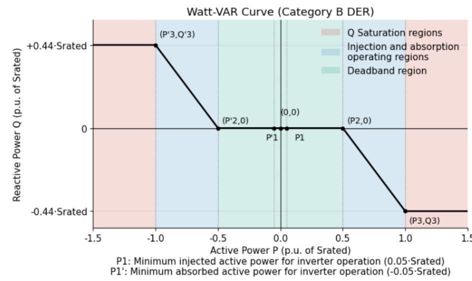

Fig. 3. Watt-VAR Curve. P: Injected active power; P': Absorbed active power

A. Constant Reactive Power Mode

In this mode, reactive power must remain constant in an established value Q_{ref}, as required by the grid operator. If the reference current amplitude exceeds the limit condition in equation (5) while supplying both the generated active power ($P^* = P_G$) and the established reactive power ($Q^* = Q_{ref}$), the reference active power must be reduced according to equation (6). This equation is derived from (4), assuming $I_{ref} = I_{\text{rated}}$.

$$P^* = \sqrt{\frac{3\,V_{L,\text{rms}}^2\,I_{\text{rated}}^2}{2} - Q_{\text{ref}}^2}. \tag{6}$$

B. Volt-VAR Mode

This mode uses a Volt-VAR curve to determine the reactive power (Q_{ref}) necessary to achieve voltage regulation according to a reference established by the grid operator. If equation (5) is exceeded, the procedure explained in the first mode will be applied.

The curve may have different slopes, deadband, and saturation regions, such as the one shown in Fig. 2, or those presented in [2] and [10]. These should be chosen appropriately according to the PCC voltage steady-state operation.

C. Constant Power Factor Mode

Here, active and reactive powers vary proportionally to maintain an established power factor (PF_{ref}) in the PCC. From basic power theory and defining $P^* = P_G$:

$$PF_{ref} = \frac{P_G}{S_n} = \frac{P_G}{\sqrt{P_G^2 + Q_{ref}^2}}. \tag{7}$$

From (7), the required reactive power is:

$$Q^* = Q_{ref} = \frac{\sqrt{(1 - PF_{ref}^2)\,P_G^2}}{PF_{ref}}. \tag{8}$$

If the resulting current exceeds (5), both P_G and Q_{ref} are scaled by a factor of k, derived from (4):

$$I_{\text{ref}} = \sqrt{\frac{2}{3}}\,\frac{\sqrt{(kP_G)^2 + (kQ_{ref})^2}}{3\,V_{L,\text{rms}}}. \tag{9}$$

Thus, from (9), k is:

$$k = \sqrt{\frac{3}{2}}\sqrt{\frac{V_{L,\text{rms}}^2\,I_{\text{rated}}^2}{(P_G)^2 + (Q_{ref})^2}}, \tag{10}$$

ensuring (5) and making $P^* = kP_G$ and $Q^* = kQ_{ref}$.

D. Watt-VAR Mode

In this mode, the reference value for the reactive power is calculated according to a Watt-VAR curve (see Fig. 3), where Q^* is a function of P^*; this means $Q^* = Q_{(P^*)}$. This curve must be chosen according to the system requirements. This mode attempts to compensate for the DER impact on the voltage, but it does not respond directly to it [10].

If the resulting current exceeds (5) when $P^* = P_G$ and $Q^* = Q_{(P_G)}$, the reference values for P^* and Q^* should be recalculated, taking into account the following equation:

$$I_{\text{ref}} = \sqrt{\frac{2}{3}}\,\frac{\sqrt{(P^*)^2 + (Q_{(\text{P}^*)})^2}}{V_{L,\text{rms}}}. \tag{11}$$

As an example, when $P_2 \leq P^* \leq P_3$ in the Watt-VAR curve (see Fig. 3), the reactive power is calculated as:

$$Q_{(\text{P}^*)} = m(P^* - P_2), \qquad m = \frac{Q_3}{P_3 - P_2}. \tag{12}$$

Replacing (12) in (11) yields a quadratic equation in P^*:

$$aP^{*2} + bP^* + c = 0, \tag{13}$$

with coefficients $a = 2 + 2m^2$, $b = -4P_2m^2$, and $c = 2P_2^2m^2 - 3V_{L,\text{rms}}^2\,I_{\text{rated}}^2$, whose solution provides the feasible P^*, ensuring current and voltage compliance.

A flowchart of the proposed algorithm is shown in Fig. 4, where the control logic for each operating mode is illustrated.

IV. Case Study and Results

The proposed algorithm is validated in MATLAB/Simulink using the system described in section II. The system is designed following [7], [11]–[13] and operates under scenarios where voltage regulation is beyond standard limits, thus requiring reactive power support.

For this study, the Volt-VAR and Watt-VAR curves were obtained from the standard [3], [10] for Category B DER. Moreover, the Thévenin equivalent emulates common medium

979-8-3315-8138-1

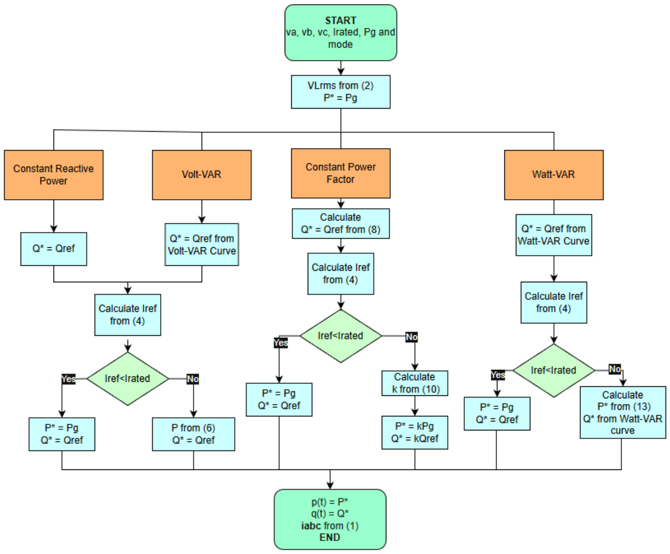

Fig. 4. Proposed algorithm flowchart

voltage grid impedance values and an X/R relationship that enables the observation of changes in voltage due to variations in active and reactive powers ($1 \leq X/R \leq 3$) [10]. The main system parameters are summarized in Table I.

TABLE I
PARAMETERS OF THE SYSTEM FOR SIMULATION TESTS

Subsystem	Values
Grid	$R_s = 25\,\text{m}\Omega,\ L_s = 110\,\mu\text{H},\ v_{grid} = 690\,\text{V}_{\text{rms}},\ f = 60\,\text{Hz}$
Inverter	$v_{dc} = 1.5\,\text{kV},\ I_{\text{rated}} = 2.36\,\text{kA},\ S_{\text{rated}} = 2\,\text{MVA}$
LCL filter	$L_1 = 30\,\mu\text{H},\ L_2 = 30\,\mu\text{H},\ C_f = 500\,\mu\text{F},\ R_f = 5\,\text{m}\Omega$
PR/LS-PWM	$K_p = 0.11,\ K_r = 175,\ f_b = 10\,\text{Hz},\ f_o = 60\,\text{Hz},\ f_{sw} = 20\,\text{kHz}$

Note: f_b and f_o denote the bandwidth and resonance frequency of the PR controller, respectively.

The algorithm's performance was evaluated for the four operating modes. During the first 0.25 seconds of all the simulation tests, reactive power control is disabled and the generator operates at rated power, i.e., $P^* = P_G = 2\text{MW}$ and $Q^* = 0$. Furthermore, the reactive power sign convention presented in the results is opposite to the one shown in Figs. 2-3, where absorbed and injected reactive power are negative and positive, respectively. The test conditions for each operating mode are presented in Table II.

The simulation results, summarized in Figs. 5–8, demonstrate the algorithm's ability to maintain standard compliance and current limitation. As shown in these figures, before 0.25 seconds—when no reactive power control is applied—the injection of active power at rated capacity causes the PCC voltage to exceed the upper limit.

In the constant reactive power mode (Fig. 5), a reactive power absorption command (Q_{ref}) is established to restore the voltage within the permissible range. The dynamic of reactive power absorption and current limitation can be seen in Fig. 5. Active power is curtailed to satisfy both the current limit and the established requirements for reactive power when $P_G = 2\text{MW}$. Once P_G decreases, the reference current falls below the limit, and curtailment is no longer necessary.

For the constant power factor mode (Fig.6), both active and reactive powers are proportionally adjusted to maintain the established power factor. It can be seen how active power curtailment increases to comply with the current limitation when the power factor decreases and the generator operates at rated power.

In the Volt–VAR mode, Fig.7 shows how reactive power improves voltage regulation while current limits are respected and the curve is followed. Nonetheless, there are scenarios where the Volt-VAR curve is not enough to reduce the voltage at the PCC to steady-state operating limits; thus, the Volt-VAR curve should be adjusted or a Volt-Watt curve must be considered to improve it [10].

Finally, the Watt–VAR mode (Fig. 8) indirectly contributes to voltage regulation, although it does not necessarily enhance it, as observed when the active power injection enters the deadband region. The results also show that the absorbed

TABLE II
SIMULATION TESTS CONDITIONS

Mode	Fig.	Time [s]	Condition
Constant Reactive Power	5	0.25–0.6	$P_g = 2\text{MW},\ Q_{\text{ref}} = 0.88\text{MVAR}$
		0.6–0.8	$P_g = 1.6\text{MW},\ Q_{\text{ref}} = 0.88\text{MVAR}$
Constant Power Factor	6	0.25–0.6	$P_g = 2\text{MW},\ PF_{\text{ref}} = 0.95$
		0.6–0.8	$P_g = 2\text{MW},\ PF_{\text{ref}} = 0.85$
		0.8–1.0	$P_g = 1.6\text{MW},\ PF_{\text{ref}} = 0.85$
Volt-VAR	7	0.25–0.5	$P_g = 2\text{MW}$
		0.5–0.7	$P_g = 1\text{MW}$
		0.7–0.9	$P_g = -0.2\text{MW}$
		0.9–1.1	$P_g = -2\text{MW}$
Watt-VAR	8	0.25–0.5	$P_g = 2\text{MW}$
		0.5–0.7	$P_g = 1\text{MW}$
		0.7–0.8	$P_g = -1\text{MW}$
		0.8–1.1	$P_g = -2\text{MW}$

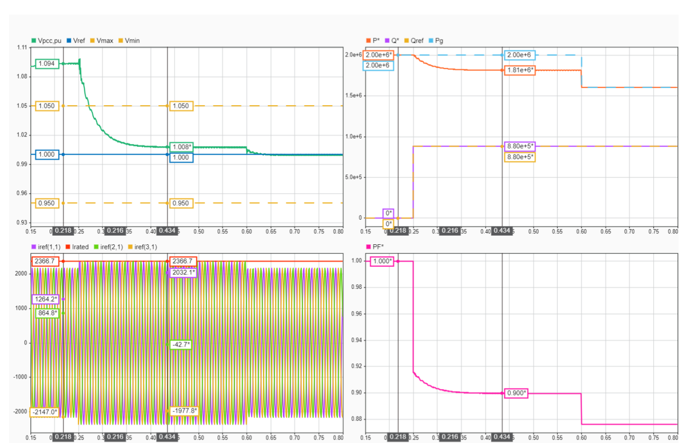

Fig. 5. Constant reactive power mode: a) PCC RMS voltage in p.u. and limits; b) Active and reactive powers; c) Reference currents and I_{rated}; d) Power factor.

979-8-3315-8138-1

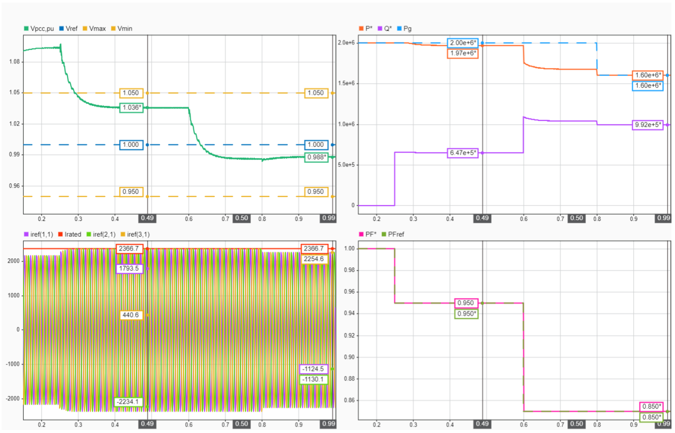

Fig. 6. Constant power factor mode: a) PCC RMS voltage in p.u. and limits; b) Active and reactive powers; c) Reference currents and I_{rated}; d) Power factor.

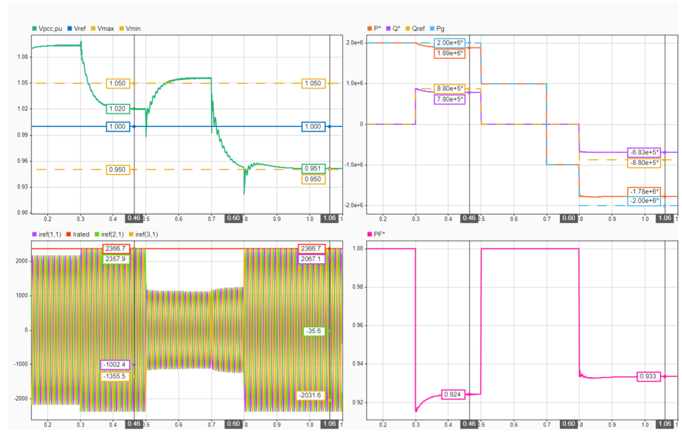

Fig. 8. Watt-VAR mode: a) PCC RMS voltage in p.u. and limits; b) Active and reactive powers; c) Reference currents and I_{rated}; d) Power factor.

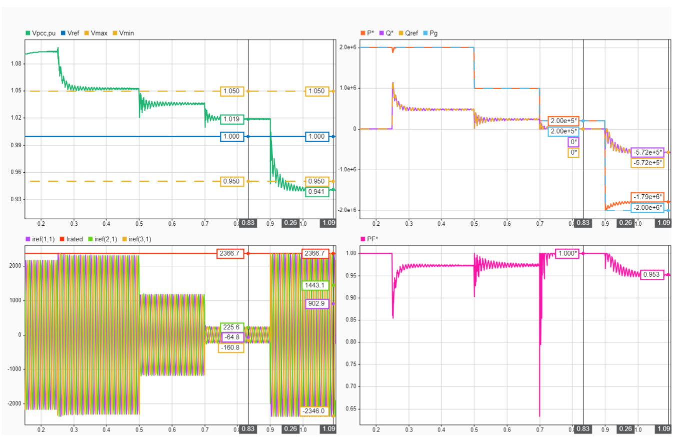

Fig. 7. Volt-VAR mode: a) PCC RMS voltage in p.u. and limits; b) Active and reactive powers; c) Reference currents and I_{rated}; d) Power factor.

active power is reduced to achieve current limitation when $P_G = -2$MW; consequently, reactive power reduction is produced due to the algorithm starting to operate in a different point of the Watt-VAR curve.

Overall, the proposed algorithm maintains the inverter current within rated limits and effectively supports voltage regulation in all analyzed scenarios.

V. Conclusions

The proposed reactive power control algorithm with current limitation provides a flexible and effective control approach for grid-connected inverters operating under the IEEE 1547-2018 modes. Unlike conventional *dq*- or $\alpha\beta$-based methods, the proposed approach directly manipulates phase currents in the *abc* frame without coordinate transformations, simplifying implementation while ensuring proper voltage and power control.

Future work will include experimental validation and the extension of the control strategy for unbalanced and distorted voltages in the PCC, as well as comparisons with *dq*- or $\alpha\beta$-based methods.

References

[1] REN21, "Renewables 2025 global status report," Paris, France, 2025, accessed: 2025-10-09. [Online]. Available: https://www.ren21.net/reports/global-status-report/

[2] R. Xu, C. Zhang, Y. Xu, Z. Dong, and R. Zhang, "Multi-objective hierarchically-coordinated Volt/Var control for active distribution networks with droop-controlled PV inverters," *IEEE Transactions on Smart Grid*, vol. 13, no. 2, pp. 998–1011, 2022.

[3] IEEE, "IEEE standard for interconnection and interoperability of distributed energy resources with associated electric power systems interfaces," *IEEE Std 1547-2018 (Revision of IEEE Std 1547-2003)*, pp. 1–138, 2018.

[4] A. Amanipoor, M. S. Golsorkhi, N. Bayati, and M. Savaghebi, "V-iq based control scheme for mitigation of transient overvoltage in distribution feeders with high PV penetration," *IEEE Transactions on Sustainable Energy*, vol. 14, no. 1, pp. 283–296, 2023.

[5] Z. Wei, Y. Sun, X. Hou, M. Su, and K. Sun, "A universal droop control for grid-connected cascaded inverters," *IEEE Transactions on Industrial Electronics*, pp. 1–6, 2025.

[6] R. Teodorescu, F. Blaabjerg, M. Liserre, and P. Loh, "Proportional-resonant controllers and filters for grid-connected voltage-source converters," *IEE Proceedings - Electric Power Applications*, vol. 153, no. 5, pp. 50 – 762, 2006.

[7] M. A. Perez, S. Ceballos, G. Konstantinou, J. Pou, and R. P. Aguilera, "Modular multilevel converters: Recent achievements and challenges," *IEEE Open Journal of the Industrial Electronics Society*, vol. 2, pp. 224–239, 2021.

[8] H. Akagi, E. H. Watanabe, and M. Aredes, *Instantaneous Power Theory and Applications to Power Conditioning*, 2nd ed. Hoboken, New Jersey: John Wiley & Sons, Inc., 2007.

[9] M. A. Mantilla, D. J. Rincón, O. Sierra, J. F. Petit, and G. Ordóñez, "Control of active and reactive powers in three phase inverters for grid-tied photovoltaic systems under unbalanced voltages," in *2014 International Conference on Renewable Energy Research and Application (ICRERA)*, 2014, pp. 583–588.

[10] IEEE, "IEEE application guide for IEEE std 1547™-2018, IEEE standard for interconnection and interoperability of distributed energy resources with associated electric power systems interfaces," *IEEE Std 1547.2-2023 (Revision of IEEE Std 1547.2-2008)*, pp. 1–291, 2024.

[11] J. Rodriguez, L. G. Franquelo, S. Kouro, J. I. Leon, R. C. Portillo, M. M. Prats, and M. A. Perez, "Multilevel converters: An enabling technology for high-power applications," *Proceedings of the IEEE*, vol. 97, no. 11, pp. 1786–1817, 2009.

[12] Y. Lang, D. Xu, S. Hadianamrei, and H. Ma, "A novel design method of LCL type utility interface for three-phase voltage source rectifier," in *2005 IEEE 36th Power Electronics Specialists Conference*, 2005, pp. 313–317.

[13] D. Jain and U. K. Kalla, "Design and analysis of LCL filter for interconnection with grid connected PV system," in *2016 IEEE 7th Power India International Conference (PIICON)*, 2016, pp. 1–6.

979-8-3315-8138-1